Journal of Power Sources 242 (2013) 91–98

Contents lists available at SciVerse ScienceDirect

Journal of Power Sources

journal homepage: www.elsevier.com/locate/jpowsour

Influence of germanium oxide addition on the electrical properties of $Li_2O–B_2O_3–P_2O_5$ glasses

Andrea Moguš-Milanković [a,*], Kristina Sklepić [a], Hrvoje Blažanović [a], Petr Mošner [b], Maryna Vorokhta [b], Ladislav Koudelka [b]

[a] Ruđer Bošković Institute, 10000 Zagreb, Croatia
[b] Department of General and Inorganic Chemistry, University of Pardubice, Faculty of Chemical Technology, 53210 Pardubice, Czech Republic

HIGHLIGHTS

- Electrical and dielectric properties of $Li_2O–GeO_2–B_2O_3–P_2O_5$ glasses were studied.
- GeO_2 addition causes the depolimerization of phosphate network.
- Formation of Li^+ conducting channels results in the el. conductivity increase.
- Subsequent conductivity drop is a consequence of more densely packed network.

GRAPHICAL ABSTRACT

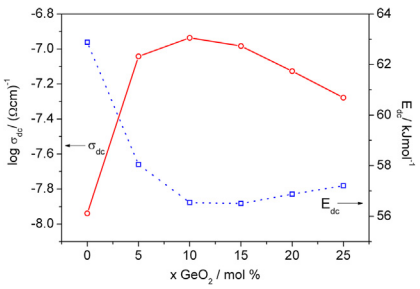

ARTICLE INFO

Article history:
Received 9 April 2013
Received in revised form
15 May 2013
Accepted 16 May 2013
Available online 24 May 2013

Keywords:
Lithium germano-phosphate glasses
Lithium ion conductivity
Electrical modulus
Dielectric relaxation

ABSTRACT

Lithium ion transport upon the addition of germanium oxide in a series of mixed glass former lithium borophosphate glasses has been investigated. The electrical and dielectric properties of $(100 - x)[0.5Li_2O–0.1B_2O_3–0.4P_2O_5]–xGeO_2$ with 0–25 mol% GeO_2 glasses have been studied over a wide temperature (183–523 K) and frequency range (0.01 Hz–1 MHz). The increase in dc conductivity with the addition of GeO_2 is attributed to the formation of ion conducting channels arising from the structural modification and formation of the P–O–Ge linkages, resulting in an easy migration of Li^+ ions along these bonds. At higher GeO_2 content glass network becomes more densely packed and ionic conductivity is slightly hindered as a consequence of the increase of bonding forces inside the network. Such a decrease in the conductivity is more reflection of the stronger cross-linkage in the glass network than that of the slight decrease in the Li^+ ion concentration. The electrical modulus formalism is used to describe the dielectric relaxation. The scaling of the ac conductivity results in an excellent collapse onto common master curve whereas the electrical modulus spectra showed slight deviation indicating the distribution of relaxation times caused by the presence of various structural units in the glass network.

1. Introduction

The need for electrolytes suitable for lithium batteries application has given rise to the investigations of numerous lithium ion based glass systems [1,2]. Glass electrolytes have certain advantages over their crystalline counterparts like physical isotropy, absence of grain boundaries and ease compositional variation [3]. Among lithium based glass electrolytes, lithium borophosphate glasses have been studied extensively in literature [4–6] because of their interesting structural and physical property changes upon network modifications. These systems contain two different glass formers (B and P) in the glass network responsible for an

* Corresponding author. Tel.: +385 1 4561 149; fax: +385 1 4680 114.
E-mail address: mogus@irb.hr (A. Moguš-Milanković).

0378-7753/$ – see front matter © 2013 Elsevier B.V. All rights reserved.
http://dx.doi.org/10.1016/j.jpowsour.2013.05.068

enhancement in the ionic conductivity. The increase in the conductivity is due to replacement of one former cation (P) by the other one (B) and formation of various borate and phosphate structural units in the glass network if the total ion concentration is kept constant. The observed behavior is usually called the "mixed glass former effect".

In this context, mixed matrix glasses of the type Li_2O–B_2O_3–P_2O_5–GeO_2 containing only a single mobile alkali ion are particularly interesting as a solid electrolyte. Recent reports [7,8] on the lithium borophosphate glasses have suggested that at fixed Li^+ ion concentration an enhancement of mobility depends on the structural and microstructural features in the glass structure. The most important structural changes are related to the presence of various structural species which varies with the borate fraction. At low boron content, up to 10 mol% B_2O_3, the increase in ionic conductivity is attributed to the formation of B-$(OP)_4$ linkage within a borophosphate glass network resulting in a larger degree of charge dispersion favorable for the ion transport. At higher boron concentration the electrical conductivity decreases due to the formation BO_3 units which could be detrimental for the Li^+ mobility. It seems that the presence of BO_3 units breaks the conduction pathways formed by BO_4 where Li^+ ions are involved as charge compensators [8].

On the other hand, with the perspective on lithium battery application, it is interesting to investigate materials for which glass composition mixing leads to the enhancement of the ionic conduction and transport characteristics. Therefore, the present work reports the investigation of the electrical properties of lithium borophosphate glasses modified by germanium oxide. Germanium oxide containing glasses are characterized by their high ion conductivity which makes them interesting candidates for solid electrolyte technology [9]. Furthermore, mixed germano-phosphate glasses have attracted considerable interest because of the possibility of fine-tuning properties with varying chemical composition [10]. Structure of alkali germano-phosphate glasses have been extensively studied by several authors using vibrational spectroscopy, ^{31}P MAS NMR spectroscopy, x-ray absorption near edge spectroscopy [11–14] and more recently by combined NMR and XPS spectroscopies [15]. These studies have suggested that alkali ions preferentially modify the phosphate units leaving the tetrahedral GeO_2 structure in the glass network unaffected [11]. It was also found [15] that the observed structural changes in sodium germano-phosphate glasses are related to the presence of a non-bridging oxygen in GeO_4 tetrahedra, which charge is compensated by sodium ions.

In our previous paper we reported a structural characterization of lithium borophosphate glasses modified by the addition of germanium oxide in the seria $(100 - x)[0.5Li_2O–0.1B_2O_3–0.4P_2O_5] - xGeO_2$ with 0–25 mol% GeO_2 [16]. The introduction of GeO_2 produces new linkages between phosphate chains through P–O–Ge bonds whose amount increases with germanium incorporation along with a depolymerization of the metaphosphate chains into pyrophosphate units. The introduction of germanium caused an increase in T_g and a decrease in the molar volume [16]. Therefore it would be interesting to examine the electrical conductivity behavior in these glasses as a function of Li_2O content.

The possibility that the germanium prefers to form tetrahedral units together with the tendency of phosphate chains to depolymerize with the addition of GeO_2 content leads to the interesting behavior in ion transport of these glasses. In this paper the influence of glass composition on electrical conductivity properties over a wide range of temperature and frequency has been studied. Furthermore, the changes in electrical conductivity and its temperature dependence have been discussed based on the completions between network breaking/forming events and Li^+ ion mobility.

2. Experimental

The detailed preparation of glasses with nominal composition $(100 - x)[0.5Li_2O–0.1B_2O_3–0.4P_2O_5] - xGeO_2$ with 0–25 mol% GeO_2, has been reported elsewhere [16]. However, it should be mentioned that the glasses were prepared from analytical grade Li_2CO_3, GeO_2, H_3BO_3 and H_3PO_4 using a total batch weight of 10 g. The homogenized starting mixture was heated slowly to 1273–1423 K in a covered Pt crucible. The melt was held at maximum temperature for 30 min and then cooled slowly in a graphite mould. Obtained glasses were annealed for 30 min at a temperature 5 K below their glass transition temperature, T_g.

Samples for electrical/dielectric property measurements were cut from annealed bars and polished. Gold electrodes, 7 mm in diameter, were sputtered onto both sides of 1 mm thick discs cut from the glass bars using Sputter Coater SC7620. The samples were stored in a dessicator until the electrical conductivity was measured. Dielectric and electrical properties were obtained by measuring complex impedance using an impedance analyzer (Novocontrol Alpha-AN Dielectric Spectrometer) over the frequency range from 0.01 Hz to 1 MHz and in the temperature range from 183 to 523 K. The temperature was controlled to an accuracy of ±0.20 K.

The complex impedance data, $Z^*(\omega)$, were plotted in the Nyquist representation form, a typical complex plane plot represented by imaginary part $Z''(\omega)$ vs. real part $Z'(\omega)$ for each temperature. A point of this curve represents a given measurements of $Z'(\omega)$ and $Z''(\omega)$, at a specific angular frequency ω ($\omega = 2\pi f$).

The impedance spectra were analyzed by means of equivalent circuits modeling and parameters were obtained by the complex non-linear least square (CNLLSQ) fitting. The complex impedance plots typical for all investigated glasses consist of a single semicircle with the center below the real axis. The equivalent circuit that represents such depressed semicircle is a parallel combination of resistor (R) and constant-phase element (CPE). The CPE is an empirical impedance function of the type $Z_{CPE}{}^* = A(j\omega)^{-\alpha}$, where A and α are the constants. The values of the resistance obtained from the fitting procedures, R and electrode dimensions (d is sample thickness and A is electrode area) were used to calculate the dc conductivity, $\sigma_{dc} = d/(R \cdot A)$.

3. Results

3.1. Electrical conductivity

The complex impedance plots for all glasses investigated exhibit a high frequency depressed semicircle and a low-frequency spur, which emanated from ion migration and the electrode polarization, respectively, Fig. 1. As the interfacial resistance increases with decreasing temperature, the low-frequency semicircle falls outside the experimental frequency range at low temperatures. The radius of the semicircle related to the bulk behavior decreases with increasing temperature indicating that the ion conduction is thermally activated, inset to Fig. 1. The intercept of the depressed semicircle on the real axis gives the value for the bulk dc resistance, R_b, offered by the sample at various temperatures. The parameters of the equivalent circuits were obtained by the complex non-linear least square fitting directly to the measured impedance data. The values of the resistance, R_b and electrode dimensions were used to calculate the dc conductivity, $\sigma_{dc} = d/(R \cdot A)$, Table 1.

The activation energy for dc conductivity, E_{dc}, for each sample was determined from the slope of $\log(\sigma_{dc} \cdot T)$ *vs.* $1/T$ using equation $\sigma_{dc}T = \sigma_o \exp(-E_{dc}/k_BT)$, where σ_{dc} is the dc conductivity, σ_o is the pre-exponent, k_B is the Boltzmann constant and T is the

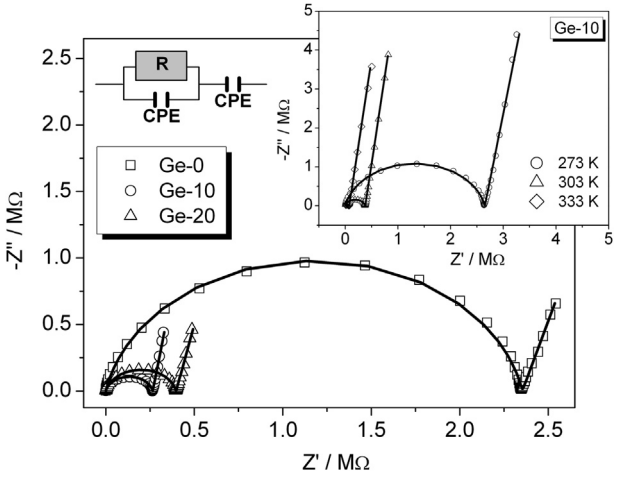

Fig. 1. Complex impedance spectra measured at 303 K for different $(100 - x)[0.5Li_2O–0.1B_2O_3–0.4P_2O_5] - xGeO_2$ glasses. Inset: complex impedance spectra for Ge-10 glass at different temperatures.

temperature (K). The activation energies, E_{dc}, for all investigated $Li_2O–B_2O_3–P_2O_5–GeO_2$ glasses are listed in Table 1.

Fig. 2 shows compositional dependence of dc conductivity, σ_{dc}, at 303 K and activation energy, E_{dc}. The dc conductivity, σ_{dc}, for glasses containing GeO_2 exhibits higher values than that for GeO_2-free glass whereas the values for E_{dc} decrease with increasing GeO_2 content. It is interesting to note that the σ_{dc} increases for about one order of magnitude for glass containing 5 mol% GeO_2 reaching the value of 9.13×10^{-8} $(\Omega\ cm)^{-1}$. Such a behavior is related to the structural modifications observed with the addition of GeO_2 as a result of interlinking between phosphate chains and germanium tetrahedral units [16]. It is assumed that the formation of mixed former network in the glass structure improves the motion of Li^+ ions. With further increase of GeO_2 content the σ_{dc} slightly decreases from 1.16×10^{-7} to 5.29×10^{-8} $(\Omega cm)^{-1}$. A more significant decrease in dc conductivity with decreasing Li_2O content from 50 to 37.5 mol% and cross-linking of phosphate units by Ge atom was expected. However, it seems that the depolymerization of phosphate units along with the incorporation of Ge atoms into the network forms continuous channels for the easier migration of Li^+ ions.

Going further in the interpretation of conductivity, the ac conductivity, σ_{ac}, at different temperatures for Ge-10 glass is shown in Fig. 3. The ac conductivity spectra, generally, show a universal feature [17] where at low-frequency region the conductivity is independent of frequency and corresponds to the dc conductivity, σ_{dc}, whereas at higher frequencies exhibits dispersion in power law fashion. The transition point, between these two regions is shifted

Table 1
Composition and selected properties for the $(100 - x)[0.5Li_2O–0.1B_2O_3–0.4P_2O_5] - xGeO_2$, $x = 0–25$ (mol%) glasses.

Sample	Glass composition (mol%)				$\sigma_{dc}/(\Omega cm)^{-1}$ [a] (±0.5%)	E_{dc}/kJ mol^{-1} (±0.5%)
	LiO_2	B_2O_3	P_2O_5	GeO_2		
Ge-0	50	10	40	0	1.15×10^{-8}	62.88
Ge-5	47.5	9.5	38	5	9.13×10^{-8}	58.04
Ge-10	45	9	36	10	1.16×10^{-7}	56.55
Ge-15	42.5	8.5	34	15	1.04×10^{-7}	56.51
Ge-20	40	8	32	20	7.50×10^{-8}	56.87
Ge-25	37.5	7.5	30	25	5.29×10^{-8}	57.20

[a] At 303 K.

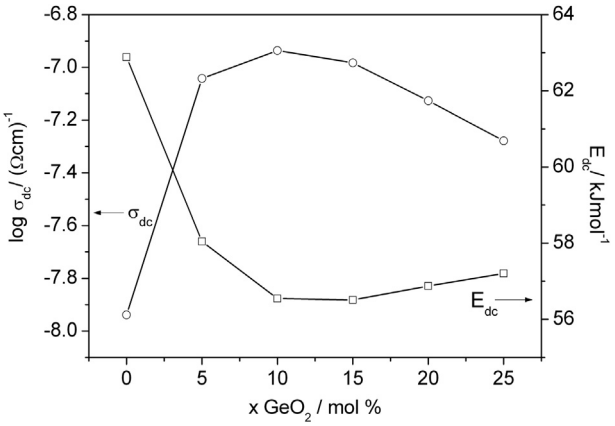

Fig. 2. The dependence of the dc conductivity, σ_{dc}, at 303 K and activation energy for dc conductivity upon GeO_2 content.

toward higher frequency with increasing temperature. The slopes observed at low-frequency region at higher temperatures are related to the electrode polarization. The ac conductivity of ionically conducting glasses over a wide range of temperatures and frequencies shows a region of power law behavior in the form [17,18]:

$$\sigma(\omega) = \sigma_{dc} + A\omega^s \quad (1)$$

where A is the temperature dependent constant and s is the power law exponent, $s < 1$. The A determines the strength of polarizability while exponent s represents the degree of interaction between mobile ions with the network. For glasses investigated in the present study the s factor slightly decreases for Ge-5 glass whereas for other glasses containing higher GeO_2 content is almost constant, inset to Fig. 4.

For better understanding of the motion of Li^+ ions the ac conductivity was scaled at different temperatures and composition into a single master curve. Since, for many glasses (ionic and electronic) the shape of conductivity, $\sigma(\omega)$, does not depend on temperature these curves can be superimposed using so called Summerfield scaling [19]. In this scaling approach, the conductivity axis is normalized by σ_{dc} and the frequency axis is normalized by the product $\sigma_{dc}T$ [20]. Thus, the master curve gives the dimensionless ac conductivity as a function of dimensionless frequency and can be referred as a time–temperature superposition principle.

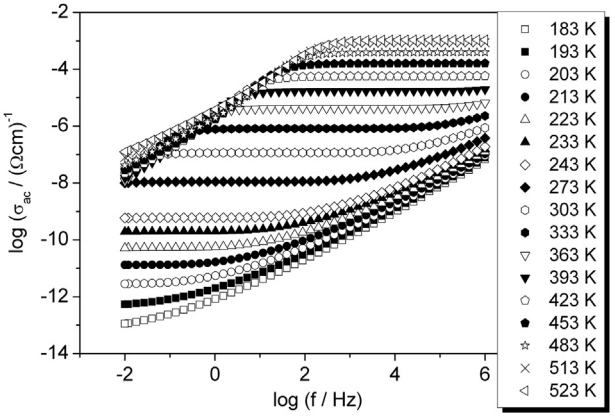

Fig. 3. Frequency dependence of the ac conductivity at different temperatures for Ge-10 glass.

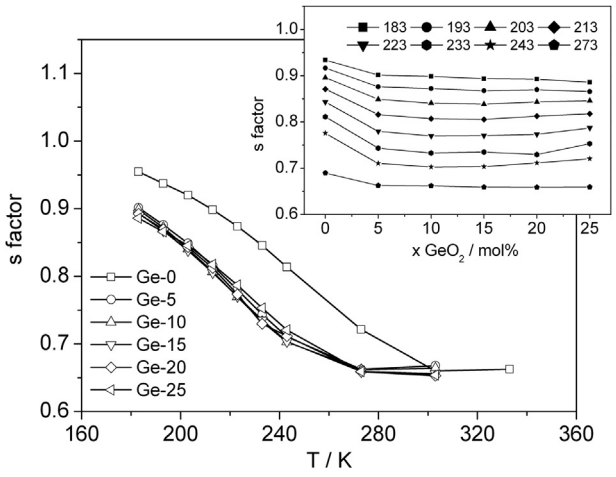

Fig. 4. Temperature dependence of s factor for different $(100 - x)[0.5Li_2O–0.1B_2O_3–0.4P_2O_5] - xGeO_2$ glasses as a function of mole fraction of GeO_2 at different temperatures.

In Fig. 5 the master curves for all glasses are shown. The conductivity isotherms of the presented glasses are superimposed onto single master curve indicating the validity of the time–temperature superposition properties. Thus the excellent time–temperature superposition indicates a common transport mechanism, which operates in the entire temperature regime.

3.2. Dielectric properties and relaxation studies

The complex permittivity $\varepsilon^*(\omega) = 1/(j\omega C_o Z^*)$ can be expressed as a complex number:

$$\varepsilon^*(\omega) = \varepsilon'(\omega) - j\varepsilon''(\omega) \quad (2)$$

where $\varepsilon'(\omega)$ and $\varepsilon''(\omega)$ are the real and imaginary parts of the complex permittivity.

The frequency dependence of the real part of the complex permittivity, $\varepsilon'(\omega)$, for Ge-10 glass at different temperatures is shown in Fig. 6(a). The values of the dielectric permittivity, $\varepsilon'(\omega)$, measured at 303 K and 11.7 Hz for the presented glasses are given in Table 2.

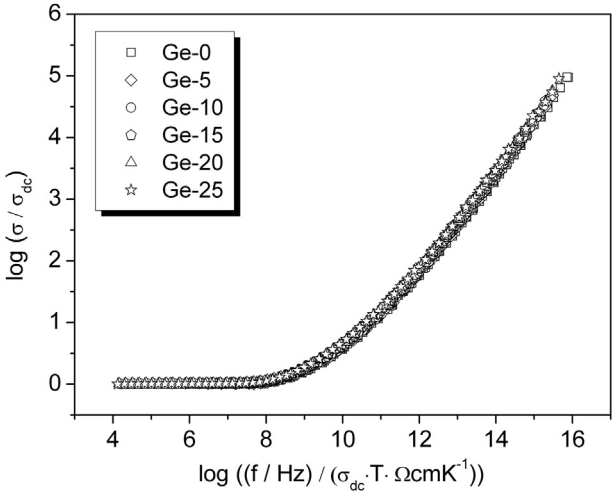

Fig. 5. Conductivity master curves for different $(100 - x)[0.5Li_2O–0.1B_2O_3–0.4P_2O_5] - xGeO_2$ glasses.

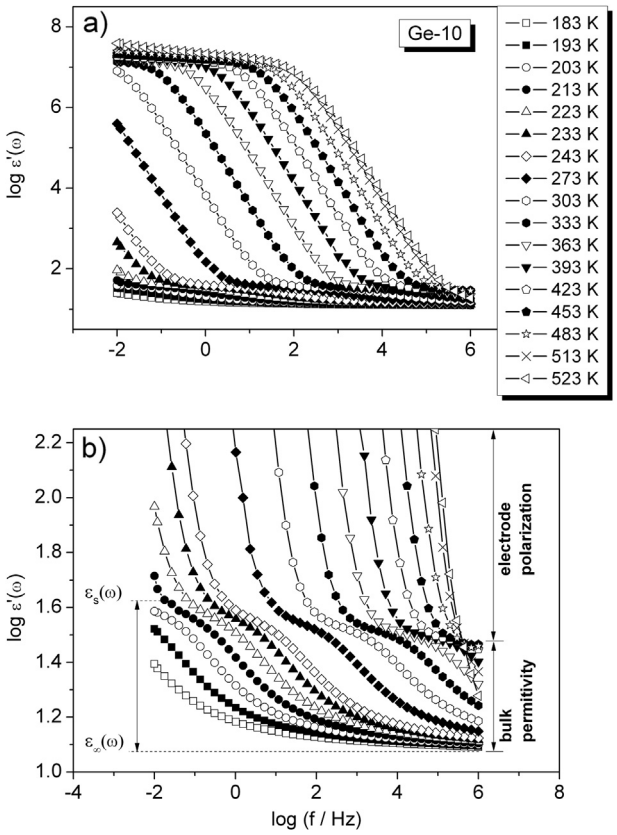

Fig. 6. (a) Frequency dependence of dielectric constant, $\varepsilon'(\omega)$ at different temperatures for Ge-10 glass. (b) Frequency dependence of dielectric constant, $\varepsilon'(\omega)$ obtained by rescaling log $\varepsilon'(\omega)$ axis.

At higher frequencies, $\varepsilon'(\omega)$ tends to approach a constant value, $\varepsilon_\infty'(\omega)$, which results from rapid polarization processes occurring in the glasses under applied field [21]. Therefore, the mobile ions will not be able to rotate sufficiently rapidly, so their oscillation will begin to lay behind this field resulting in a decrease of dielectric permittivity, $\varepsilon'(\omega)$. With increasing temperature and decreasing frequency, $\varepsilon'(\omega)$ increases considerably due to electrode polarization. The bulk polarization of the glass sample results from the presence of metallic electrodes, which do not permit transfer of the mobile ions into external circuit. Consequently, ions are accumulated near the electrodes causing large polarization of the glass. It should be noted that the electrode polarization sometimes masks the low-frequency permittivity of glass samples. However, for glasses studied in this paper, the low-frequency plateau, ε_s, denoted as the low-frequency static value, usually associated with the polarization effects of the long range hopping of mobile ions with respect to the immobile glass matrix in the ionic glasses, is

Table 2
Selected dielectric properties for the $(100 - x)[0.5Li_2O–0.1B_2O_3–0.4P_2O_5] - xGeO_2$, $x = 0–25$ (mol%) glasses.

Sample	$\varepsilon'(\omega)$[a] (±0.5%)	$\Delta\varepsilon'(\omega)$ at 303 K	$\tau_{M''}$/s (±0.5%)	$f_{0M''}$/Hz (±0.5%)	$E_{M''}$/kJ mol^{-1} (±0.5%)
Ge-0	30.06	14.8	8.58×10^{-5}	4.56×10^{13}	62.63
Ge-5	132.13	16.2	1.11×10^{-5}	5.57×10^{13}	57.63
Ge-10	123.59	18.4	9.82×10^{-6}	3.33×10^{13}	56.05
Ge-15	104.23	20.3	1.12×10^{-5}	3.40×10^{13}	56.27
Ge-20	93.54	21.0	1.40×10^{-5}	3.30×10^{13}	56.35
Ge-25	68.71	22.9	2.03×10^{-5}	1.90×10^{13}	56.59

[a] At 303 K and 11.7 Hz.

well-defined as can be seen in Fig. 6(b). The static permittivity, ε_s, was determined by diminishing log $\varepsilon'(\omega)$ scale which allows the separation of the bulk permittivity from the electrode polarization.

The magnitude of the bulk polarization called dielectric strength, is given by $\Delta\varepsilon = \varepsilon_s(\omega) - \varepsilon_\infty(\omega)$ as proposed by Sidebottom [22]. The dielectric strength, $\Delta\varepsilon$, represents the rate of permittivity change due to the relaxation. For glasses studied in this paper, the well-defined plateau, ε_s, makes it possible to determine the permittivity changes and the correlation effects between successful hops.

Fig. 7 exhibits the systematic increase in $\Delta\varepsilon$ values with the addition of GeO_2 as a result of the enhanced Li^+ ion mobility. For all glasses, the $\Delta\varepsilon$ shows a temperature dependence, which agrees well with data obtained for other phosphate glasses [23]. The inset to Fig. 7 exhibits the dependence of $\Delta\varepsilon$ upon the GeO_2 content at three different temperatures.

The temperature dependence of $\varepsilon'(\omega)$ measured at 11.7 Hz for all glasses is shown in Fig. 8. It can be seen that the $\varepsilon'(\omega)$ is less dependent of temperature at lower temperatures whereas increases at higher temperatures. For GeO_2-free glass the values for $\varepsilon'(\omega)$ are lower than that for glasses containing GeO_2 in the whole temperature region. Values for $\varepsilon'(\omega)$ measured at 303 K and 11.7 Hz for all glasses are given in Table 2.

The factor, which means the phase difference due to the loss of energy within the sample at a particular frequency is the loss factor tangent, $\tan\delta = \varepsilon''(\omega)/\varepsilon'(\omega)$. The frequency dependence of $\tan\delta$ at different temperatures for Ge-10 glass is shown in Fig. 9. The maximum in the $\tan\delta$ peak shifts to higher frequency as the temperature increases indicating a thermally activated behavior. Nature of the variation of the dielectric parameters with frequency and temperature is found to be similar for all the other glasses in this study. Generally, the dielectric losses at high frequencies are much lower than those occurring at low frequencies at specific temperature. This kind of dependence of $\tan\delta$ upon frequency is typically associated with losses by conduction.

An alterative formalism that may be used for analyzing electrical relaxation behavior in glasses is the electrical modulus model [24]. Although there is a debate [25] about the suitability of this model, the advantage of this representation is that the electrode polarization effects are minimized in this formalism [26]. In the modulus formalism, an electric modulus $M^*(\omega)$ is defined in terms of the reciprocal of the complex dielectric constant $\varepsilon^*(\omega)$ as:

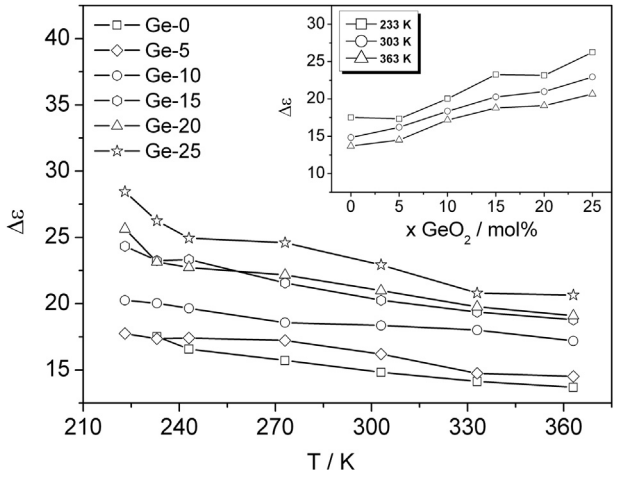

Fig. 7. Temperature dependence of $\Delta\varepsilon$ for different $(100 - x)[0.5Li_2O–0.1B_2O_3–0.4P_2O_5] - xGeO_2$ glasses. Inset: dependence of $\Delta\varepsilon$ upon GeO_2 content at different temperatures.

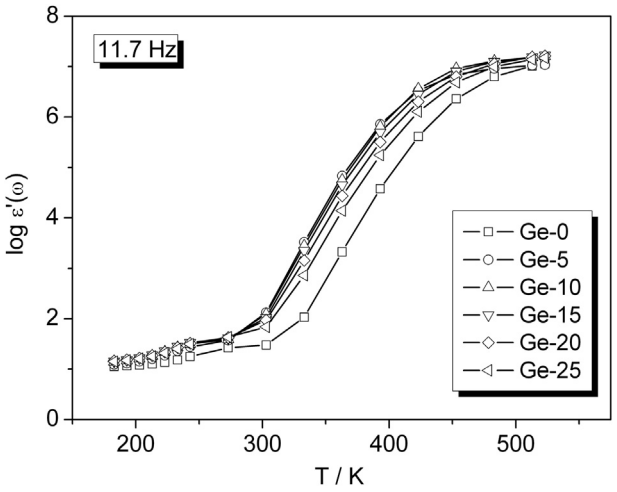

Fig. 8. Temperature dependence of dielectric constant, $\varepsilon'(\omega)$ at 11.7 Hz for different $(100 - x)[0.5Li_2O–0.1B_2O_3–0.4P_2O_5] - xGeO_2$ glasses.

$$M^*(\omega) = 1/\varepsilon^*(\omega) = \varepsilon'(\omega)/(\varepsilon'(\omega))^2 + (\varepsilon''(\omega))^2 + i\varepsilon''(\omega)/(\varepsilon'(\omega))^2 + (\varepsilon''(\omega))^2 = M'(\omega) + iM''(\omega) \quad (3)$$

The frequency dependence of $M''(\omega)$ at different temperatures for GeO_2 glass is presented in Fig. 10. The maximum in the $M''(\omega)$ peak shifts to higher frequencies with increasing temperature. The frequency region below peak maximum $M''(\omega)$ determines the range in which Li^+ ions are mobile on long distances. At frequencies above peak maximum $M''(\omega)$, the carriers are spatially confined to potential wells, being mobile on short distances making only localized motion within the wells. From the characteristic frequency, which is equal to the relaxation frequency at which the maximum $M''(\omega)$, occurs, given by $\omega_{max} = 1/\tau_M = \sigma_{dc}/\varepsilon_0\varepsilon_\infty'(\omega)$, the conductivity relaxation time, τ_M, can be extracted as shown in Fig. 10. It is clear, that at any chosen temperature, τ_M for GeO_2 glasses exhibits lower values, whereas τ_M for GeO_2-free glass is almost one order of magnitude higher. The relaxation times, τ_M, for the glasses measured at 303 K, are shown in Table 2.

The scaling analysis can also be performed using the electrical modulus formalism. The normalized imaginary part of electrical modulus, $M''(\omega)/M''(\omega)_{max}$ versus f/f_{max}, for all glasses studied is scaled to the single plot, as it is shown in Fig. 11. In this figure, two regions are distinguished. In the region bellow $M''(\omega)$ peak where

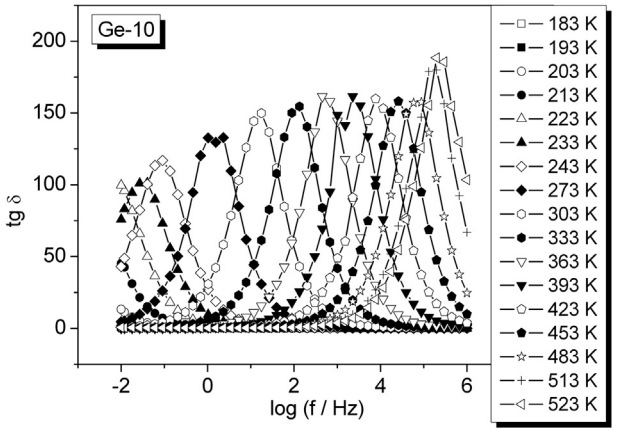

Fig. 9. Frequency dependence of dielectric loss, $\tan\delta$, at different temperatures for Ge-10 glass.

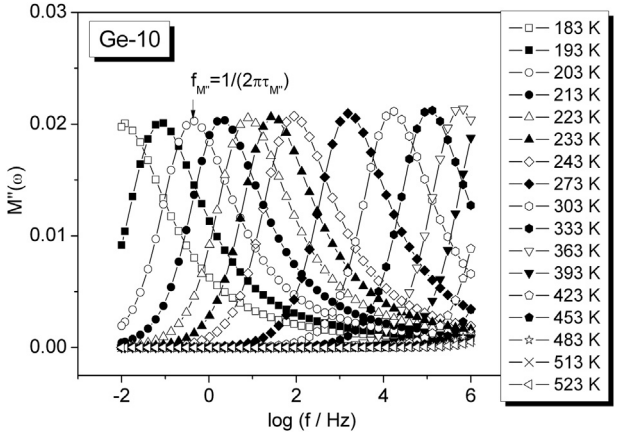

Fig. 10. Frequency dependence of electrical modulus, $M''(\omega)$, at different temperatures for Ge-10 glass.

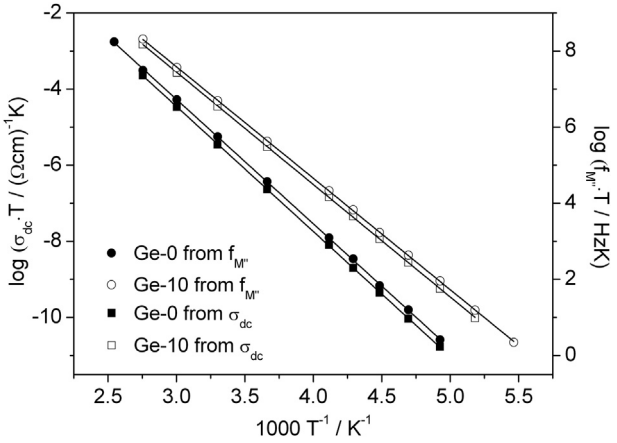

Fig. 12. Temperature dependence of the dc conductivity, σ_{dc}, and the relaxation frequency, $f_{M''}$, for the Ge-0 and Ge-10 glasses.

dc conductivity dominates all points lay on the master curve. The high frequency region is associated with decay of field where ions are spatially confined to potential wells and free to move within the wells. However, the slight deviation from muster curve at high frequencies is observed.

The plot of the relaxation frequency, $f_{M''} = 1/(2\pi\tau_{M''})$ versus $1/T$ is represented by an Arrhenius equation, $f_{M''}T = f_{oM''}\ \exp(-E_{M''}/kT)$, where $E_{M''}$ is the activation energy for the electrical relaxation. The activation energy, $E_{M''}$, determined from the slope of the log $f_{M''}T$ vs. $1/T$ for Ge-0 and Ge-10 glasses is exhibited in Fig. 12 and is given in Table 2 for all glasses. The activation energy values for the electrical modulus, $E_{M''}$, and for the dc conductivity, E_{dc}, are almost identical, suggesting that the relaxation processes and dc conductivity are in close agreement.

4. Discussion

In the previous paper [16] the effects of germanium addition on the glass forming characteristic and structure of lithium borophosphate glasses have been shown. The structural investigation exhibits that the glass structure can be regarded as a network of various phosphate and borate units interlinked via four-coordinated germanium. The addition of germanium dioxide results in the strengthening of bonds within the structural network of the modified glasses, as revealed from a substantial increase of their glass transition temperatures. It was also found that the incorporation of germanate units into borophosphate network is accompanied by the formation of P–O–Ge and Ge–O–B bonds. Therefore, according to the ^{31}P NMR and Raman spectra, the addition of GeO_2 breaks the metaphosphate chains and consequently turns metaphosphate into shorter pyrophosphate structure [16].

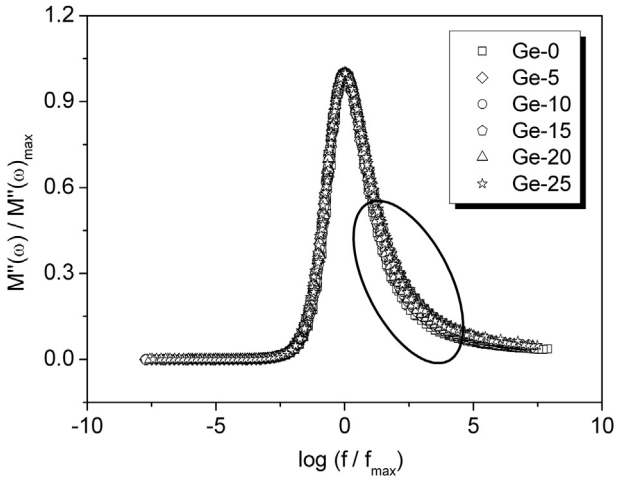

Fig. 11. Electrical modulus, $M''(\omega)$, master curves for different $(100 - x)[0.5Li_2O–0.1B_2O_3–0.4P_2O_5] - xGeO_2$ glasses.

The increase in dc conductivity can be interpreted in terms of the above mentioned modifications of glass structure. Recently it was reported [6,8,15,16] that at low B_2O_3 content a lithium borophosphate glass is predominantly composed of metaphosphate chains connected by barely detectable tetrahedral BO_4 units. Thus, it seems that in GeO_2-free glass, the glass matrix hinders the Li^+ motion which results in the lowest dc conductivity. Clearly, the anionic metaphosphate units behave as deep Coulomb traps where Li^+ ions are probably bounded to the discrete non-bridging oxygens [7].

On the other hand with addition of GeO_2, the reactivity between germanium and phosphate units induces an increase in number of germanate units incorporated into phosphate network, leading to the formation of pyrophosphate units. However, it was shown [15,16] that one of the oxygen atom bound to the Ge atom in tetrahedrally coordinated GeO_4 units is a non-bridging. So, it seems that glass modifier Li^+ ions are shared between these two glass former units where Li^+ ions are involved in the charge compensation of $[GeO_4]^-$ units, whose charge is more delocalized. Such a behavior increases the mobility of Li^+ ions since widely dispersed charges through P–O–Ge linkages modify the bonding of Li^+ ions which are thus trapped less effectively. Moreover, it is well known that the depolymerization of the metaphosphate chains and the increase in the amount of pyrophosphate units which contain non-bridging oxygens enhances the electrical conductivity of glasses [27,28].

As the germanium content increases, $x > 10$, the dc conductivity slightly decreases as a result of further incorporation of germanate structural units into the glass network leading to the increase of the network reticulation by the formation of P–O–Ge and Ge–O–Ge bonds. Moreover, the presence of large amount of germanate units increases the anionic character of the germanium groups which reduces the Li^+ ions mobility and breaks the conduction pathways. However, it is worth mentioning that with increasing GeO_2 content small amount of BO_3 units, 8% of the total number of boron units, is also formed that might reduce the Li^+ ions mobility [16].

The observed frequency dependence of ac conductivity is in accordance with the jump relaxation model [29,30]. In this model, at low frequencies, a mobile ion jumps successfully to its neighboring vacant site due to a long time period available and such successive jumps result in a long range translational motion of ions contributing to the dc conductivity. Once an ion has completed its initial hop from initial site to the neighboring site, two competing relaxation processes can be viewed at higher frequencies, the ion may hop back to its initial position (correlated forward-backward hopping) or the neighborhood may relax with respect to the newly occupied sites. Either one of these competing ways of relaxation can be characterized by respective rate. Thus, an increased probability of the correlated forward-backward hopping at higher frequency along with the relaxation leads to the observed high frequency conductivity dispersion.

Considering the conductivity behavior using power law, the exponent s which represents the degree of interaction between mobile ions with the network can be given by the ratio:

$$s = \text{initial back} - \text{hope rate}/\text{initial state} - \text{relaxation rate}$$

The term initial back-hope describes the motion of a hopping ion to its initial site. This movement is due to the Coulomb repulsive interaction between mobile ions and can be explained as follows. The site relaxation is the shift from the site of potential minimum to the position of the hopping ion due to the rearrangement of neighboring ions. The diminution of the Coulomb interaction between mobile ions with the decrease of their concentrations reduces the back-hope rate leading to a decrease in s [31]. For glasses investigated in the present study the s factor slightly decreases for Ge-5 glass whereas for other glasses containing higher GeO_2 content is almost constant, inset to Fig. 4. This leads to the conclusion that with the addition of GeO_2 more unstable ion sites are formed which, due to the opening of many channels, results in an efficient ion transport over long distances. It seems that the mobile Li^+ ions are less constricted by surrounding oxide network which contains borate, phosphate and germanate units. This can be attributed to the number of channels available for ion transport, i.e. to the dimensionality of ion transport pathways. Clearly, oxygen coordination around germanium which possesses larger degree of charge dispersal and serves as Li^+ ions compensating sites is responsible for the modification of the local environment that could mimic changes to the dimensionality of the conduction space [32].

The variations of s values as a function of temperature for all glasses are plotted and exhibited in Fig. 4. There is a decreasing trend in s values as temperature increases. The most apparent in Fig. 4 is the increase in exponent s which occurs at temperatures below 270 K. According to Sidebottom [33] the increase at low temperature is attributed to the transition to a second dielectric process where ionic motion is less active. However, the origin of this process is still uncertain and therefore will not be discussed in this paper. On the other hand the process at high temperatures is related to the ionic relaxation. For glasses in this series the exponent s at high temperature plateau, at about 300 K, has a value $s = 0.65 \pm 0.04$, which is consistent with "universal" $s = 0.67 \pm 0.03$ for many alkali oxide glasses [34].

Summerfield law was a basis for scaling properties, which allows obtaining a universal conductivity curve. As shown in Fig. 5 the ac conductivity for all glasses investigated is found to be scaled very well. The data collapse to a common curve, implying that exponent s is independent of GeO_2 content, which is in accordance to the present findings. This suggests that there is a good time–temperature superposition and that the conduction mechanism remains unchanged with addition of GeO_2.

In general, the relaxation phenomena in various ion conducting glasses are observed to be non-Debye type [35,36]. The non-Debye behavior arises from the distribution of ionic sites within the glassy matrix to which the ionic jump occurs. Thus, for ionically conducting glasses it is assumed that the ions interact strongly with the network. It is worth noting that this is related to the long range hoping of ions from one site where they are effectively trapped to the others where polarization is associated with the changing environment of different sites ions hops into. Therefore, the conduction and conduction-related polarization are integrated into single continuous process [25].

For glasses investigated, the decrease in $\varepsilon'(\omega)$ and $\varepsilon''(\omega)$ with increasing GeO_2 content in glass network is attributed to the conductivity changes, which are directly related to the enhancement in Li^+ ions mobility for Ge-5 and Ge-10 glasses and slight reduction for glasses containing higher GeO_2 content. It was previously noted that the incorporation of germanate units into phosphate network, at higher GeO_2 content, reticulates the phosphate chains and leads to a more cross-linked network. As a consequence, such a structure is more suitable for ion trapping which reduces the overall ionic diffusion and causes a decrease in the conductivity.

It was mentioned earlier that the $\Delta\varepsilon$ is a quantity, which depends on ion hopping, and its changes are related to the changes in hopping dynamics of the mobile Li^+ ions [25]. The values of $\Delta\varepsilon$ shown in Fig. 7 indicate a progressive increase with increasing GeO_2 content in glasses. It seems that this increase is related to the changes in the glass structure, suggesting that the $\Delta\varepsilon$ depends on the structural modifications which are responsible for the formation of many channels available for favorable ion transport where Li^+ ions are less effectively trapped. This is consistent with previous reports [23,25] where it has been demonstrated that the $\Delta\varepsilon$ is related to the hopping dynamics, i.e. to the concentration of mobile ions. Our analysis clearly leads to the conclusion that the $\Delta\varepsilon$ depends not only upon the population of mobile ions but also on the modification of glass network which contains structural units with lower charge density that support an easy migration of Li^+ ions.

The conductivity relaxation model, where a dielectric modulus is defined by $M^*(\omega) = 1/\varepsilon^*(\omega)$, can provide information about the relaxation mechanisms [24]. According to the earlier discussion, two apparent relaxation regions appeared, the low-frequency region, being associated with the hopping conduction and high frequency region being attributed to the relaxation polarization process.

The relaxation times, $\tau_{M''}$, as calculated from the frequency at the $M''(\omega)$ maximum, shown in Fig. 10 and listed in Table 2, are thermally activated with following respective activation energies, $E_{M''}$. From Table 2, it is clear that the relaxation times, $\tau_{M''}$, for the presented glasses decrease as the GeO_2 content increases, if compared to the GeO_2-free glass, due to the higher E_{dc} and consequently, a lower conductivity, σ_{dc}. For Ge-10 glass, the relaxation time, $\tau_{M''}$, becomes the lowest, which causes the highest conductivity in this glass.

The scaling of modulus data has been carried out in order to test whether the relaxation process remains unchanged or not throughout the compositions and temperature range studied. Fig. 11 shows the resulting master curve obtained for different glass compositions exhibiting a good overlap for all spectra on a master curve. However, at high frequencies the curves do not collapse to a common muster curve. Such a behavior could depend on details of the short time dynamics where mismatch relaxation includes relaxation movements or adjustments of the glass network and is influenced by the local structure. Similar scaling behavior is observed for other glasses [23]. Sidebottom [23] proposed that such behavior can be correlated to the dimensionality of the local cation conduction space in the sense that by depolarization of phosphate

chains and incorporation of germanate into glass network, local environment becomes constricted leading to the dispersion in shorter time region. This is consistent with a slight decrease in *s* factor and decrease in the free volume of the glasses containing GeO_2. Clearly, the divergences in the scaled data for these glasses probably originated from the difference in the distribution of relaxation times caused by the structural disorder in the glass network.

As already mentioned, the temperature dependence of the relaxation times for these glasses is a thermally activated process following Arrhenius law. The activation energies, $E_{M''}$, and E_{dc}, observed in the temperature range measured for all glasses are almost identical as can be seen in Tables 1 and 2. This behavior suggests that the same activation energy and existence of a single carrier are related to the same relaxation process.

5. Conclusions

The effect of compositional changes observed by the addition of GeO_2 to the $Li_2O–B_2O_3–P_2O_5$ glass on the electrical conductivity and dielectric properties has been investigated. The observed increase in dc conductivity with addition of GeO_2 is attributed to the formation of ion conducting channels arising from the structural modification and formation of the P–O–Ge linkages, resulting in an easy migration of Li^+ ions along these bonds. The maximum in the Li^+ conductivity can be attributed to the presence of various structural units interlinked by tetrahedral germanium units. At higher GeO_2 content glass network becomes more densely packed and ionic conductivity is slightly hindered as a consequence of the increase of bonding forces inside the network. The reticulation of the glass network is primarily a result of the incorporation of GeO_2 units into phosphate chains by forming more Ge–O–Ge linkages which favor Li^+ trapping ability. This trapping mechanism causes a slight reduction in the overall ionic conductivity. Such a decrease in the conductivity is more a reflection of the stronger cross-linkage in the glass network than that of the slight decrease in the lithium concentration.

Finally, the addition of the third glass former to the glass network has a direct impact on the changes of conductivity through the formation of mixed structural units which serve as compensating sites for lithium ions.

The dielectric permittivity, $\varepsilon'(\omega)$, and its variations with temperature and frequency have been analyzed on the basis of the dielectric relaxation processes. The electrical modulus formalism is used to describe the conductivity relaxation. The scaling of the ac conductivity results in an excellent collapse onto common master curve whereas the electrical modulus spectra showed slight deviation indicating the distribution of relaxation times caused by the presence of various structural units in the glass network.

Acknowledgments

This work was supported by the Croatian Ministry for Science, Education and Sport. Grant No: 098-0982929-2916. The Czech authors are grateful for the financial support from the Grant Agency of the Czech Republic (Grant No. 13-00355S).

References

[1] M. Duclot, J.-L. Souquet, J. Power Sources 97–98 (2010) 610–615.
[2] A.G. Ritchie, J. Power Sources 136 (2004) 285–289.
[3] R.C. Agrawal, R.K. Gupta, J. Mater. Sci. 34 (1999) 1131–1162.
[4] A. Magistris, G. Chiodelli, M. Villa, J. Power Sources 14 (1985) 87–91.
[5] B.K. Money, K. Hariharan, Solid State Ionics 179 (2008) 1273–1277.
[6] F. Muñoz, L. Montagne, L. Pascual, A. Durán, J. Non-Cryst. Solids 355 (2009) 2571–2577.
[7] M. Storek, R. Böhmer, S.W. Martin, D. Larink, H. Eckert, J. Chem. Phys. 137 (2012), 124507/1–124507/12.
[8] B. Raguenet, G. Tricot, G. Silly, M. Ribes, A. Pradel, J. Mater. Chem. 21 (2011) 17693–17704.
[9] N.K. Karan, B. Natesan, R.S. Katiyar, Solid State Ionics 177 (2006) 1429–1436.
[10] B.V.R. Chowdari, G.V. Subba Rao, G.Y.H. Lee, Solid State Ionics 136 (2000) 1067–1075.
[11] S. Kumar, S. Murugavel, K.J. Rao, J. Phys. Chem. B 105 (2001) 5862–5873.
[12] M.R. Sahar, A. Wahab, M.A. Hussein, R. Hussin, J. Non-Cryst. Solids 353 (2007) 1134–1140.
[13] G.S. Henderson, R.T. Amos, J. Non-Cryst. Solids 328 (2003) 1–19.
[14] H.M. Wang, G.S. Henderson, J. Non-Cryst. Solids 354 (2008) 863–872.
[15] J. Ren, H. Eckert, J. Phys. Chem. C 116 (2012) 12747–12763.
[16] P. Mošner, M. Vorokhta, L. Koudelka, L. Montagne, B. Revel, K. Sklepić, A. Moguš-Milanković, J. Non-Cryst. Solids, accepted for publication.
[17] A.K. Jonscher, Dielectric Relaxation in Solids, Chelsea Dielectric Press, London, 1996.
[18] D.P. Almond, A.R. West, R. Grant, J. Solid State Commun. 44 (1982) 1277–1280.
[19] S. Summerfield, Philos. Magn. B 52 (1985) 9–22.
[20] B. Roling, A. Happe, K. Funke, M.D. Ingram, Phys. Rev. Lett. 78 (1997) 2160–2163.
[21] C.J.F. Böttcher, P. Bordewijk, Theory of Electrical Polarization, vol. 2, Elsevier, Amsterdam, 1978.
[22] D.L. Sidebottom, J. Zang, Phys. Rev. B 62 (2000) 5503–5507.
[23] D.L. Sidebottom, Phys. Rev. B 61 (2000) 14507–14516.
[24] P.B. Macedo, C.T. Moynihan, R. Bose, Phys. Chem. Glasses 13 (1972) 171–179.
[25] D.L. Sidebottom, B. Roling, K. Funke, Phys. Rev. B 63 (2000), 024301/1–024301/7.
[26] A. Šantić, C.W. Kim, D.E. Day, A. Moguš-Milanković, J. Non-Cryst. Solids 356 (2010) 2699–2703.
[27] S. Kumar, K.J. Rao, Solid State Ionics 170 (2004) 191–199.
[28] A. Moguš-Milanković, A. Šantić, S.T. Reis, K. Furić, D.E. Day, J. Non-Cryst. Solids 342 (2004) 97–109.
[29] K. Funke, Solid State Ionics 18–19 (1986) 183–190.
[30] K. Funke, B. Roling, M. Lange, Solid State Ionics 105 (1998) 195–208.
[31] C. Cramer, K. Funke, B. Roling, T. Saatkamp, D. Wilmer, M.D. Ingram, A. Pradel, M. Ribes, G. Taillades, Solid State Ionics 86–88 (1996) 481–486.
[32] J.C. Dyre, P. Maass, D.L. Sidebottom, Rep. Prog. Phys. IOP Sci. 72 (046501) (2009) 1–19.
[33] D.L. Sidebottom, J. Non-Cryst. Solids 255 (1999) 67–77.
[34] D.L. Sidebottom, P.F. Green, R.K. Brow, J. Non-Cryst. Solids 183 (1995) 151–160.
[35] R. Böhmer, K.L. Ngai, C.A. Angell, D.J. Plazek, J. Chem. Phys. 99 (1993) 4201–4209.
[36] J.C. Dyre, J. Appl. Phys. 64 (1988) 2456–2468.